Wavelet approximation-based affine invariant shape representation functions. IEEE Trans PAMI

Article *in* IEEE Transactions on Pattern Analysis and Machine Intelligence · March 2006

Impact Factor: 5.78 · DOI: 10.1109/TPAMI.2006.43 · Source: PubMed

3 authors:

Ibrahim El rube
Taif University
32 PUBLICATIONS **239** CITATIONS
SEE PROFILE

Maher Ahmed
Wilfrid Laurier University
38 PUBLICATIONS **320** CITATIONS
SEE PROFILE

Mohamed S. Kamel
University of Waterloo
497 PUBLICATIONS **7,020** CITATIONS
SEE PROFILE

Wavelet Approximation-Based Affine Invariant Shape Representation Functions

Ibrahim El Rube', *Student Member*, *IEEE*,
Maher Ahmed, and
Mohamed Kamel, *Fellow*, *IEEE*

Abstract—In this paper, new wavelet-based affine invariant functions for shape representation are presented. Unlike the previous representation functions, only the approximation coefficients are used to obtain the proposed functions. One of the derived functions is computed by applying a single wavelet transform; the other function is calculated by applying two different wavelet transforms with two different wavelet families. One drawback of the previously derived detail-based invariant representation functions is that they are sensitive to noise at the finer scale levels, which limits the number of scale levels that can be used. The experimental results in this paper demonstrate that the proposed functions are more stable and less sensitive to noise than the detail-based functions.

Index Terms—Wavelet transform, shape representation, affine transformation, invariants.

1 Introduction

Shape representation is a pivotal step in shape analysis and matching systems. After the shape is located and segmented from an image, a representation technique is used to efficiently characterize the shape. The complexity and the performance of the subsequent steps in shape analysis systems are largely dependent on the invariance, robustness, stability, and uniqueness of the applied shape representation technique. In the past decade, several techniques have been proposed for 2D shape representation and matching. They include curvature scale space (CSS) [1], [2], [3], fuzzy-based matching [4], dynamic programming [5], shape contexts [6], shock graphs [7], geodesic paths [8], Fourier descriptors [9], and wavelet descriptors [10].

Objects can be recognized by their color, texture, and shape. Shape descriptors have become more popular, since they were adopted in the MPEG-7 system [11]. Region, contour, and skeleton shape descriptors were evaluated under the MPEG-7 system using a single-shape data set [12]. Generally, contour-based descriptors performed significantly better than other category descriptors [13], [3].

Recent work in the area of extracting wavelet features which are invariant to geometric transformations has been very promising [14]. Wavelet analysis has become a powerful tool in several disciplines, including shape analysis and recognition [15], [16], [17]. Many researchers have adopted the Wavelet Transform (WT) in shape representation and matching. For example, WT was applied in 2D domains in [18], [19], [20], and [21], whereas WT was applied to 1D shape boundary in [22], [23], [24], and [10]. Due to the spatial and frequency localization property of the wavelet basis functions, wavelet descriptors are more efficient in representing and describing shapes than Fourier descriptors and moments [10].

The remainder of this paper is organized into the following sections: Section 2 is a brief overview of related research. In Sections 3 and 4, the proposed functions and the experimental results are presented, respectively. Last, the study is summarized and suggestions for future work are given.

- *I. El Rube' is with the Systems Design Engineering Department, University of Waterloo, 200 University Avenue West, Waterloo, Ontario, Canada N2L 3G1. E-mail: ibrahim@pami.uwaterloo.ca.*
- *M. Ahmed is with the Physics and Computer Science Department, Wilfrid Laurier University, 75 University Avenue West, Waterloo, Ontario, Canada N2L 3C5. E-mail: mahmed@wlu.ca.*
- *M. Kamel is with the Electrical and Computer Engineering Department, University of Waterloo, 200 University Avenue West, Waterloo, Ontario, Canada N2L 3G1. E-mail: mkamel@pami.uwaterloo.ca.*

Manuscript received 24 Sept. 2003; revised 29 Dec. 2004; accepted 21 June 2005; published online 13 Dec. 2005.
Recommended for acceptance by B. Kimia.
For information on obtaining reprints of this article, please send e-mail to: tpami@computer.org, and reference IEEECS Log Number TPAMI-0287-0903.

2 Related Work

In this section, previously published papers in which the WT has been used to obtain affine invariant shape representations from its contour are reviewed. Previous affine invariant wavelet-based shape boundary representations have been based on the detail coefficients, and the functions will be given next.

Alferez and Wang [25] have proposed geometric and illumination invariants that depend on the wavelet detail coefficients for object recognition. Also, the authors have demonstrated that more complicated invariant functions can be constructed from more than two wavelet detail scale levels.

Tieng and Boles [26], [27], [28], [29] have derived more than one affine invariant representation function by applying the dyadic WT to the contour of the shape. In [26], [27], Tieng and Boles have developed a relative invariant function from the approximation and detail coefficients of the shape contour that is mathematically expressed as

$$I_1(i,k) = A_i\tilde{\boldsymbol{x}}_k D_i\tilde{\boldsymbol{y}}_k - A_i\tilde{\boldsymbol{y}}_k D_i\tilde{\boldsymbol{x}}_k, \tag{1}$$

where $A_i\tilde{\boldsymbol{x}}_k$ are the approximation coefficients of the distorted boundary sequence $\tilde{\boldsymbol{x}}_k$ and $D_i\tilde{\boldsymbol{y}}_k$ are the detail coefficients of the distorted boundary sequence $\tilde{\boldsymbol{y}}_k$. For classification purposes, only the two levels with the highest energy concentrations are selected.

Another invariant function was calculated by Tieng and Boles using the complex Daubechies wavelet functions [28]. The real and imaginary parts of the detail coefficients have been used to compute this function.

By using the wavelet detail coefficients of two different wavelet functions, Tieng and Boles have developed another invariant function [29]. This function is given by

$$I_2(j,k) = D_j^1\tilde{\boldsymbol{x}}_k D_j^2\tilde{\boldsymbol{y}}_k - D_j^1\tilde{\boldsymbol{y}}_k D_j^2\tilde{\boldsymbol{x}}_k, \tag{2}$$

where $D_j^1\tilde{\boldsymbol{x}}_k$ and $D_j^1\tilde{\boldsymbol{y}}_k$ are the detail coefficients of the distorted boundary at scale level j using the first wavelet transform and $D_j^2\tilde{\boldsymbol{x}}_k$ and $D_j^2\tilde{\boldsymbol{y}}_k$ are the detail coefficients of the distorted boundary after the second wavelet transform is applied at scale level j.

Also, Khalil and Bayoumi have derived a wavelet-based affine invariant function by using a dyadic wavelet transform [30], [31], [32]. The invariant function, the detail-detail representation function, is computed from the detail coefficients generated by the wavelet transform of the shape boundary. The basic relative invariant function, with only two dyadic scale levels, is defined as

$$I_3(i,j,k) = D_i\tilde{\boldsymbol{x}}_k D_j\tilde{\boldsymbol{y}}_k - D_i\tilde{\boldsymbol{y}}_k D_j\tilde{\boldsymbol{x}}_k, \tag{3}$$

where $D_i\tilde{\boldsymbol{x}}_k$ and $D_i\tilde{\boldsymbol{y}}_k$ are the detail coefficients of the affine transformed sequences x_k and y_k at scale levels i and j, respectively.

In [33], Bala and Cetin proposed a computationally efficient method for computing Khalil's detail-based invariant functions by utilizing the decimated wavelet transform.

In [31], Khalil and Bayoumi have continued their previous work that is described in [30]. The invariant functions are computed by using two, three, or four dyadic scale levels.

Khalil and Bayoumi have derived an absolute wavelet-based conic invariant function that uses all the detail scale levels (except

the first two), which increases the discrimination power of the invariant function [32].

From this review, it is evident that all the representation functions are based on the detail coefficients. One problem of these is that the amplitudes of the first few levels are small and highly sensitive to noise. To overcome this problem, these levels are avoided when computing the detail-based invariant functions. Another problem is that these functions are unstable when the wavelet family, used to compute the detail coefficients, changes.

In this paper, new affine invariant functions for shape representation are introduced to overcome these problems. The proposed functions are derived from the wavelet approximation coefficients of the shape boundary by applying either one or two different wavelet transforms.

3 Wavelet-Based Affine Invariant Shape Representation Functions

The framework for deriving affine invariant representation functions from the wavelet decomposition consists of the following steps:

The shape boundary (sometimes called the shape outer contour) is found and extracted by using one of the known boundary tracing techniques (the 8-connectivity technique is used in this work). The parameterized shape boundary $c_k = [x_k, y_k]$ is split into two 1D sequences, x_k and y_k.

For a 2D shape represented by its contour parametric equation (sequences x_k and y_k) and subjected to an affine transformation, the relation between the original and the distorted sequences is given by

$$\begin{bmatrix} \tilde{\boldsymbol{x}}_k \\ \tilde{\boldsymbol{y}}_k \end{bmatrix} = \begin{bmatrix} c_{11} & c_{12} \\ c_{21} & c_{22} \end{bmatrix} \begin{bmatrix} x_k \\ y_k \end{bmatrix} + \begin{bmatrix} b_1 \\ b_2 \end{bmatrix}, \tag{4}$$

where $\tilde{\boldsymbol{x}}_k$, $\tilde{\boldsymbol{x}}_k$ are the affine distorted sequences c_{11}, c_{12}, c_{21}, and c_{22} denote the affine matrix coefficients, and b_1 and b_2 represent the translation parameters. The effect of the translation parameters is easily reduced by normalizing the shape boundary centroid. The normalization is completed by subtracting the mean value of the boundaries from their extracted values.

From the wavelet multiresolution analysis properties [34], and for any function $f(k) \in L^2(R)$, $f(k)$ can be expressed by the approximation and detail wavelet coefficients

$$f(k) = \sum_n A_{J,n}\phi_{J,n}(k) + \sum_{j=j_o}^{J}\sum_n D_{j,n}\psi_{j,n}(k) \;\; J > j_o, \tag{5}$$

where $A_{J,n}$ are the approximation coefficients at scale level J, $\phi_{J,n}(k)$ is the scaling function, $D_{j,n}$ are the detail coefficients at scale level j, $\psi_{j,n}(k)$ is the wavelet function, and j_o is the finest decomposed scale level. For simplicity, the wavelet coefficients will be written without the suffix n (e.g., $A_{j,n}$ and $D_{j,n}$ will be denoted as A_j and D_j, respectively). More detailed explanations of the wavelet transform theory and its applications are found in [15], [34], and [35].

If the WT is applied to the affine distorted shape boundary, then the wavelet transformed shape boundary is affected by the same affine transformations. This occurs because the WT is a linear transform and the same affine transformation exists in the wavelet domain (after the translation effect has been removed).

For the two different representations of x_k and y_k (i.e., by using either different scale levels or two types of different coefficients), all the wavelet coefficients (in all the scale levels) are subjected to the same geometric transformation,

$$\begin{bmatrix} WT_i\tilde{\boldsymbol{x}}_k & WT_j\tilde{\boldsymbol{x}}_k \\ WT_i\tilde{\boldsymbol{y}}_k & WT_j\tilde{\boldsymbol{y}}_k \end{bmatrix} = \begin{bmatrix} c_{11} & c_{12} \\ c_{21} & c_{22} \end{bmatrix} \begin{bmatrix} WT_i x_k & WT_j x_k \\ WT_i y_k & WT_j y_k \end{bmatrix}. \tag{6}$$

An affine invariant function is computed by taking the determinant of (6), which is

$$\begin{aligned} &WT_i\tilde{\boldsymbol{x}}_k WT_j\tilde{\boldsymbol{y}}_k - WT_i\tilde{\boldsymbol{y}}_k WT_j\tilde{\boldsymbol{x}}_k = \\ &\det(C)(WT_i x_k WT_j y_k - WT_i y_k WT_j x_k), \end{aligned} \tag{7}$$

where C is the transformation matrix. Most of the previously derived affine invariant representation functions [32], [25], [31], [26], [27], [30] can be computed from (7). These invariant functions are computed by selecting the wavelet coefficients WTx_k and WTy_k as either the wavelet detail coefficients [32], [25], [31], [30] or the approximation and detail coefficients [26], [27].

3.1 Invariant Representation Function Using One Wavelet Transform

In this investigation, a function that is less sensitive to the small variations in the finer decomposed levels is developed by considering only the approximation coefficients. From (7), if only the approximation coefficients are used (i.e., WTx_k and WTy_k are replaced by Ax_k and Ax_k, respectively), then an approximation-approximation representation function equals

$$I_4(i,j,k) = A_j\tilde{\boldsymbol{x}}_k A_i\tilde{\boldsymbol{y}}_k - A_i\tilde{\boldsymbol{x}}_k A_j\tilde{\boldsymbol{y}}_k, \tag{8}$$

where $A_j\tilde{\boldsymbol{x}}_k$, $A_i\tilde{\boldsymbol{x}}_k$ are the distorted approximation coefficients of x_k at scales j and i. This function is a relative invariant function (due to the existence of the determinant $det(C)$). It can be easily shown that (8) is equivalent to

$$\begin{aligned} I_4(i,j,k) =&[(A_i\tilde{\boldsymbol{x}}_k \star \check{\boldsymbol{h}}_j)A_i\tilde{\boldsymbol{y}}_k - A_i\tilde{\boldsymbol{x}}_k(A_i\tilde{\boldsymbol{y}}_k \star \check{\boldsymbol{h}}_j)] \\ &+[(D_i\tilde{\boldsymbol{x}}_k \star \check{\boldsymbol{g}}_j)A_i\tilde{\boldsymbol{y}}_k - (D_i\tilde{\boldsymbol{y}}_k \star \check{\boldsymbol{g}}_j)A_i\tilde{\boldsymbol{x}}_k], \;\; j = i+1, \end{aligned} \tag{9}$$

where $\check{\boldsymbol{h}}_j$ and $\check{\boldsymbol{g}}_j$ are the impulse responses of the synthesis low pass and high pass filters, respectively.

Two distinct terms are included in (9): the approximation-approximation term and the approximation-detail term. The performance of this function depends on the scale levels and the filters used in decomposing the sequences. For the finer scale levels, the first part almost vanishes and the second part dominates, which indicates that this function behaves like the approximation-detail function in the finer scale levels.

3.2 Invariant Representation Function Using Two Wavelet Transform

Another invariant function from the approximation coefficients is developed by applying (7) and two different wavelet transforms with different wavelet basis functions. Therefore,

$$I_5(i,j,k) = A_j^1\tilde{\boldsymbol{x}}_k A_i^2\tilde{\boldsymbol{y}}_k - A_i^2\tilde{\boldsymbol{x}}_k A_j^1\tilde{\boldsymbol{y}}_k. \tag{10}$$

The selection of any two scale levels for computing this function depends on the arrangement of the applied wavelet families. The first wavelet is denoted by WT1 and the second one by WT2. Then, calculating a single invariant function from two different scales by taking the first scale from WT1 and the second scale from WT2 yields a different function than selecting the reverse order sequence. This is due to the different behavior of the wavelet families when they are applied to the same signal. The selection of the order sequence is subject to the application and sensitivity of the wavelet families to noise and other artifacts. Another choice is to select $i = j$ which yields a function from different wavelet families at the same scale level. This function is useful when studying the behavior of the shapes at specific levels since the function does not combine two different scale levels. The total number of representation functions that can be obtained from (10) is L^2, where L is the total number of the obtained wavelet scale levels. For single wavelet transform functions (i.e., (8)), only $L(L-1)/2$ functions can be obtained.

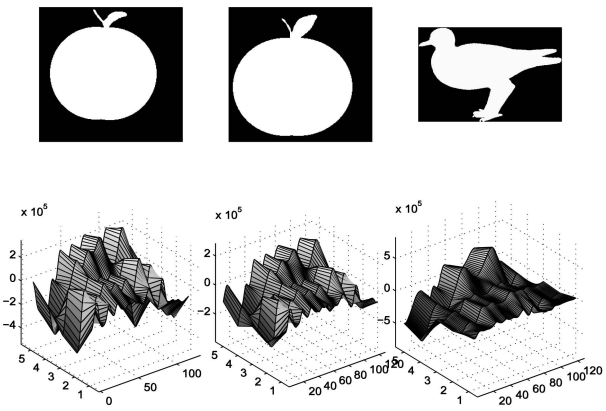

Fig. 1. The upper row, from left to right, shows three shapes: apple-1, apple-12, and bird-1. The invariant functions I_5 are shown below each of them.

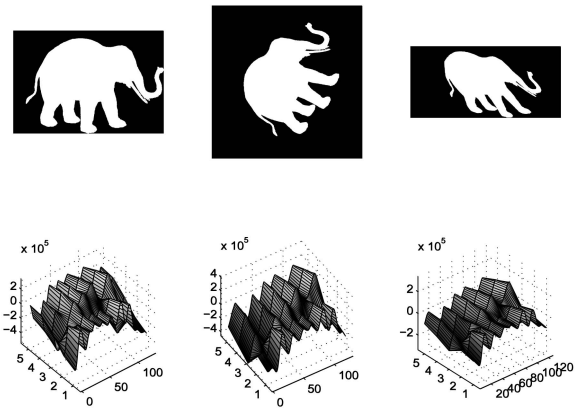

Fig. 2. The upper row, from left to right, shows three shapes: original, rotated, and skewed. The invariant functions I_5 are shown below each of them.

Consequently, the advantage of using two different wavelet transforms with different basis functions is that the discrimination between the shapes increases. This occurs because of the increase in the number of invariant representation functions that can be obtained from applying two different wavelets. In addition, the development of higher order invariant functions by using four (or more) different scale levels is facilitated.

The functions in this paper are relative invariants and are computed to be absolute invariants by dividing these functions by another relative function(s) or by dividing these functions by any significant (nonzero) value from the same function (e.g., the maximum value).

4 Experimental Results

In order to test the new invariant representation functions, the MPEG-7 CE-shape-1 data set is chosen for the experiment. This data set consists of 1,400 shapes, grouped in 70 classes. The shapes are derived from: natural objects, man-made objects, objects extracted from cartoons, and manually drawn objects.

Two experiments are described in this section. The first experiment compares the proposed functions with the related wavelet-based functions. In the second experiment, a method, based on the derived representation functions, is tested. The results of the second experiment are compared with those of the MPEG-7 test experiments [3].

4.1 Testing the Proposed Functions against Other Wavelet-Based Invariant Functions

The functions that are tested in this study are (8) and (10). In addition, they are compared to the detail-based functions given in (1), (2), and (3). Fig. 1 and Fig. 2 illustrate the invariant function I_5, plotted for the different shapes. The total number of shapes for this experiment is 210. Thirty-five original shapes from the different classes of the MPEG-7 data set are distorted by applying the affine transformation to the original 2D shapes. The translation parameters are removed by calculating and subtracting the centroid of the shape. As a result, each group consists of one original shape and five rotated, skewed, or scaled shapes. Fig. 2 shows a sample of these shapes.

The parameters in this experiment are: scale $\in [1, 0.7]$, $\theta \in [0, 30^o, 60^o]$, and skew $\in [0, 0.4, 0.6]$. All the shapes in this experiment are resampled to 128 points so that the WT decomposes each of the sequences x_k and y_k into seven different scale levels.

In addition, the normalized cross-correlation function adopted in [25] and [32] is used in the experiment to measure the similarities between any two invariant functions. For the two sequences a_k and b_k, the normalized cross-correlation is

$$R_{ab}(l) = \frac{\sum_l \sum_k a_k b_{k-l}}{\sqrt{\sum_k a_k^2 \sum_k b_k^2}}. \tag{11}$$

Since the cross-correlation is not translation invariant, one of the sequences, a_k or b_k, is rendered periodically; then, the maximum value of the correlation is selected. Such an arrangement reduces the effect of the boundary starting point variation on the calculations.

In [27], Tieng and Boles have proved that the B-spline wavelet functions perform better for single wavelet function than other wavelets. In this paper, the quadratic spline wavelet is used in the single wavelet functions. For the two wavelet functions, Table 1 shows that the quadratic and Daubechies (db8) wavelets perform better than the other combinations.

4.1.1 Applying Different Wavelet Families

Table 1 lists the performance results of all the invariant representation functions used in this paper's experiment. The average of the maximum cross-correlation values is computed for the scale levels one to four. Although changing the first wavelet family affects all the invariant functions, changing the second

TABLE 1
The Average Performance of All the Invariant Functions Used in the Experiment Computed for Scale Levels from One to Four

Inv. function	I_1	I_3	I_4
qbspline	98.51 %	97.60 %	98.30 %

Inv. function	I_2	I_5
qbspline+db8	84.19 %	98.08 %
db8+qbspline	84.19 %	97.68 %
qbspline+coif3	86.17 %	97.57 %
coif3+qbspline	86.17 %	96.62 %

TABLE 2
The Average Performance of All the Invariant Functions in the Presence of Noise

Inv. Function	I_1	I_2	I_3	I_4	I_5
40.38 db	95.53 %	84.06 %	94.31 %	97.12 %	95.79 %
34.40 db	91.31 %	67.46 %	83.80 %	94.90 %	95.16 %
28.89 db	82.20 %	58.13 %	74.11 %	91.49 %	91.49 %
25.62 db	77.02 %	52.80 %	69.44 %	85.45 %	87.24 %
22.80 db	69.94 %	48.02 %	64.02 %	79.42 %	83.63 %

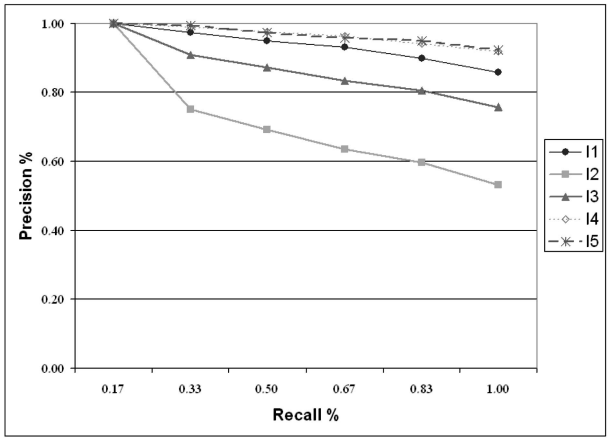

Fig. 3. Average precision-recall for all the invariant functions with SNR= 34.4db.

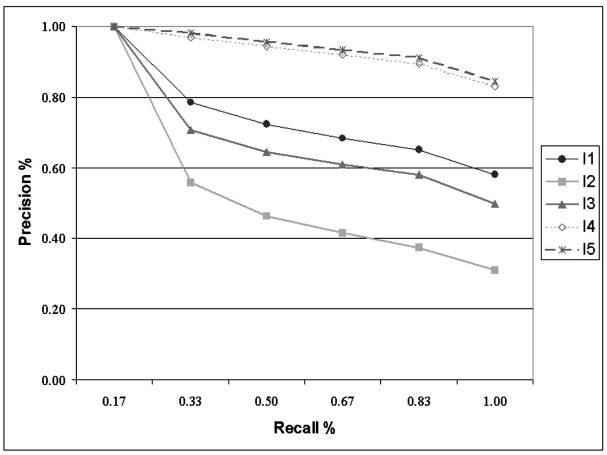

Fig. 4. Average precision-recall for all the invariant functions with SNR= 22.8db.

wavelet family affects only I_2 and I_5. The results indicate that using the qbspline with the db8 is slightly better than using the qbspline with the coif3 wavelet.

4.1.2 *Testing the Invariant Functions with Shapes Corrupted by Noise*

To measure the robustness of the invariant functions against noise, different noise levels are added to the shapes. The average SNR for each noise test is: 40.38 db, 34.4 db, 28.89 db, 25.62 db, and 22.8 db, respectively.

Table 2 exhibits the performance of all the invariant functions, computed for the noisy shapes, by using quadratic spline with Daubechies (db8) wavelets. In general, the results in these two tables show that the detail-dependent functions are more affected by noise than the approximation-approximation functions.

The average precision-recall curves are plotted for the invariant functions at different scale levels. The curves in Fig. 3 and Fig. 4 reflect the stability of the proposed functions over that of the detail-based functions for noise levels 34.4db and 22.8db, respectively.

It is evident from the results in Table 1, Table 2, Fig. 3, and Fig. 4 that the approximation-approximation functions, typically, outperform the detail-based invariant representation functions, especially in the finer scale levels. From the results obtained so far, the following is observed:

- In general, the approximation-approximation representation functions outperform the detail-based representation functions. More specifically, function I_5 has the highest performance of all the functions, even if different wavelet families are utilized.
- The invariant representation function obtained by adopting the quadratic spline and the Daubechies wavelets perform better than the function obtained by using the quadratic spline and the Coiflet wavelets.
- The invariant functions that are computed by two wavelet transforms are more stable than those with only one wavelet transform.

The approximation-approximation projective invariant representation functions can be easily computed and obtained by employing the cross-ratio or any other method for obtaining the projective invariants. Moreover, the methods of Alferez and Wang [25] and Khalil and Bayoumi [30], [32], [31] for obtaining projective invariant functions can be employed for obtaining the projective invariant approximation-approximation representation functions.

4.2 Comparison with Other MPEG-7 Tested Descriptors

In this section, another experiment is conducted using the MPEG-7 data set by performing similarity-retrieval, scaling, rotation, and nonrigid tests. For the first three tests, the 1,400 MPEG-7 shapes are used, whereas, for the nonrigid test, the 1,100 marine animal shapes with the 200 frames of the bream fish swimming back and forth are used. The MPEG-7 Core Experiment test parameters in [3] and [12] are also used in this paper.

TABLE 3
Comparison of the Representation Methods Using the MPEG-7 Data Set

Representation	Similarity	Scaling	Rotation	Non-rigid	Overall
The proposed method	80.49 %	96.94 %	99.25 %	94.00 %	90.86 %
*CSS(optimized)	81.12 %	92,86 %	100.0 %	95.00 %	90.85 %
*CSS	79.15 %	91.03 %	100.0 %	96.00 %	90.22 %
*Wavelet	67.76 %	88.04 %	97.46 %	93.00 %	86.93 %
*ART	68.34 %	97.60 %	100.0 %	92.00 %	86.40 %
*Fourier	68.18 %	86.35 %	100.0 %	85.50 %	82.28 %
Shape Context [6]	76.51 %	-	-	-	-
Fuzzy [4]	76.51 %	-	-	-	-

The results of the items with asterisks are taken from [3].

Several authors tried to compare their methods to the MPEG-7 descriptors. In order to be compared with these techniques, a method based on the proposed affine invariant functions I_4 and I_5 is implemented as follows:

- In the first stage, the average of the combinations that compute the invariant function I_5 is calculated. Then, the normalized cross-correlations are computed between each query shape and the data set. The computations are performed for the functions: the positive, the negative, and the flipped functions. The best K*N matched shapes in each direction are selected, where K is an arbitrary number chosen in order to speed up the calculations without affecting the retrieval performance and N is the number of shapes in the class (K=10 is found to be more convenient for similarity-retrieval).
- In the second stage, the same method described above is applied for the selected shapes by computing the normalized cross-correlations for the function I_4 at all scale levels.

The method used in the CSS for calculating the global parameters is also adopted in this experiment. The results obtained from the proposed method, illustrated in Table 3, show a comparable performance with the techniques tested in the MPEG-7 system. The similarity retrieval rate can be increased by asymmetrically matching the invariant functions of the shapes in the data set at all the scale levels.

5 Conclusions

In this paper, affine invariant shape representation functions based on the approximations of the shape boundary are derived. To compute these functions, either one or two wavelet transforms are used. The application of two different wavelet transforms expands the number of invariant functions that can be obtained and provides the opportunity to select more robust functions. The experimental results prove that the derived approximation-approximation functions are less sensitive to noise than the detail-based functions. Also, the results indicate that the use of two transforms is not the best choice for the detail-detail representation function. On the contrary, the performance of the approximation-approximation representation functions, by using two wavelets, yields better results. The results obtained from a method based on the proposed functions exhibits a comparable performance with the results of the techniques tested in the MPEG7 system. Future work should focus on enhancing the similarity-based retrieval performance by employing the affine invariant representation functions. The similarity retrieval rate can be increased by adopting an asymmetrical measure (using Hausdorff-like distance) and matching the invariant functions of the shapes in the data set at all the scale levels.

Acknowledgments

This research is supported by the Natural Sciences and Engineering Research Council (NSERC) of Canada.

References

[1] F. Mokhtarian and A. Mackworth, "A Theory of Multiscale, Curvature-Based Shape Representation for Planar Curves," *IEEE Trans. Pattern Analysis and Machine Intelligence*, vol. 14, no. 8, pp. 789-805, Aug. 1992.

[2] S. Abbasi and F. Mokhtarian, "Affine-Similar Shape Retrieval: Application to Multiview 3-D Object Recognition," *IEEE Trans. Image Processing*, vol. 10, no. 1, pp. 131-139, Jan. 2001.

[3] F. Mokhtarian and M. Bober, *Curvature Scale Space Representation: Theory, Applications, and MPEG-7 Standardization.* Kluwer Academic Publishers, 2003.

[4] Y. Chen and J. Wang, "A Region-Based Fuzzy Feature Matching Approach to Content-Based Image Retrieval," *IEEE Trans. Pattern Analysis and Machine Intelligence*, vol. 24, no. 9, pp. 1252-1267, Sept. 2002.

[5] E. Petrakis, A. Diplaros, and E. Milios, "Matching and Retrieval of Distorted and Occluded Shapes Using Dynamic Programming," *IEEE Trans. Pattern Analysis and Machine Intelligence*, vol. 24, no. 11, pp. 1501-1516, Nov. 2002.

[6] S. Belongie, J. Malik, and J. Puzicha, "Shape Matching and Object Recognition Using Shape Contexts," *IEEE Trans. Pattern Analysis and Machine Intelligence*, vol. 24, no. 24, pp. 509-522, Apr. 2002.

[7] T. Sebastian, P. Klein, and B. Kimia, "Recognition of Shapes by Editing Their Shock Graphs," *IEEE Trans. Pattern Analysis and Machine Intelligence*, vol. 26, no. 5, pp. 550-571, May 2004.

[8] E. Klassen, A. Srivastava, W. Mio, and S. Joshi, "Analysis of Planar Shapes Using Geodesic Paths on Shape Spaces," *IEEE Trans. Pattern Analysis and Machine Intelligence*, vol. 26, no. 3, pp. 372-383, Mar. 2004.

[9] T. Bui and G. Chen, "Multiresolution Moment-Wavelet-Fourier Descriptor for 2-D Pattern Recognition," *Proc. SPIE-The Int'l Soc. for Optical Eng.*, vol. 3,078, pp. 552-557, 1997.

[10] G. Chauang and C. Kuo, "Wavelet Descriptor of Planar Curves: Theory and Applications," *IEEE Trans. Image Processing*, vol. 5, no. 1, pp. 56-70, Jan. 1996.

[11] Jose M. Martinez, "Mpeg-7 Overview (Version 9)," Technical Report ISO/IEC JTC1/SC29/WG11N5525, ISO/IEC JTC1/SC29/WG11, Int'l Organization for Standardization, Coding of Moving Pictures and Audio, Mar. 2003.

[12] M. Bober, "Mpeg-7 Visual Shape Descriptors," *IEEE Trans. Circuits and Systems for Video Technology*, vol. 11, no. 6, pp. 716-719, Jan. 2001.

[13] L. Latecki, R. Lakamper, and U. Eckhardt, "Shape Descriptors for Non-Rigid Shapes with a Single Closed Contour," *Proc. IEEE Conf. Computer Vision and Pattern Recognition (CVPR)*, pp. 424-429, 2000.

[14] R. Brooks, L. Grewe, and S. Iyengar, "Recognition in the Wavelet Domain: A Survey," *J. Electronic Imaging*, vol. 10, no. 3, pp. 757-784, July 2001.

[15] S. Mallat, *A Wavelet Tour of Signal Processing*, second ed. Academic Press, 1999.

[16] L. Costa and R. Cesar Jr., *Shape Analysis and Classification, Theory, and Practice.* CRC Press LLC, 2001.

[17] M. Sonka, V. Hlavac, and R. Boyle, *Image Processing Analysis and Machine Vision.* PWS Publishing, 1999.

[18] M. Mandal, S. Panchanathan, and T. Aboulnasr, "Illumination Invariant Image Indexing Using Moments and Wavelets," *J. Electronic Imaging*, vol. 7, no. 2, pp. 282-293, Apr. 1998.

[19] Y. Tang and J. Liu, "Wavelet-Based Rotationally Invariant Target Classification," *SPIE, Signal Processing, Sensor Fusion, and Target Recognition*, vol. 3,068, no. 6, pp. 102-112, Apr. 1997.

[20] L. Feng and T.D. Bui, "Classification of Similar 2-D Objects by Wavelet-Sparse-Matrix (WSM) Method," *Int'l J. Pattern Recognition and Artificial Intelligence*, vol. 15, no. 2, pp. 329-345, Mar. 2001.

[21] D. Shen and H. Ip, "Discriminative Wavelet Shape Descriptors for Recognition of 2-D Patterns," *Pattern Recognition*, vol. 32, pp. 151-165, 1999.

[22] Q. Tieng and W. Boles, "Recognition of 2-D Object Contours Using the Wavelet Transform Zero-Crossing Representation," *IEEE Trans. Pattern Analysis and Machine Intelligence*, vol. 19, no. 8, pp. 910-916, Aug. 1997.

[23] K. Tsang, "Recognition of 2-D Standalone and Occluded Objects Using Wavelet Transform," *Int'l J. Pattern Recognition and Artificial Intelligence*, vol. 15, no. 4, pp. 691-705, 2001.

[24] R. Kashi, P. Bhoi-Kavde, R. Nowakowski, and T. Papathomas, "2-D Shape Representation and Averaging Using Normalized Wavelet Descriptors," *Simulation*, vol. 66, no. 3, pp. 164-178, Mar. 1996.

[25] R. Alferez and Y. Wang, "Geometric and Illumination Invariants for Object Recognition," *IEEE Trans. Pattern Analysis and Machine Intelligence*, vol. 21, no. 6, pp. 505-536, June 1999.

[26] Q. Tieng and W. Boles, "An Application of Wavelet Based Affine Invariant Representation," *Pattern Recognition Letters*, vol. 16, no. 12, pp. 1287-1296, Dec. 1995.

[27] Q. Tieng and W. Boles, "Wavelet Based Affine Invariant Representation: A Tool for Recognizing Planar Objects in 3-D Space," *IEEE Trans. Pattern Analysis and Machine Intelligence*, vol. 19, no. 8, pp. 846-857, Aug. 1997.

[28] Q. Tieng and W. Boles, "Complex Daubechies Wavelet Based Affine Invariant Representation for Object Recognition," *Proc. IEEE Int'l Conf. Image Processing*, vol. 1, pp. 198-202, 1994.

[29] Q. Tieng and W. Boles, "Object Recognition Using an Affine Invariant Wavelet Representation," *Proc. Second Australian and New Zealand Conf. Intelligent Information Systems*, pp. 307-311, 1994.

[30] M. Khalil and M. Bayoumi, "Affine Invariant Object Recognition Using Dyadic Wavelet Transform," *Proc. 2000 Canadian Conf. Electrical and Computer Eng.*, vol. 1, pp. 421-425, 2000.

[31] M. Khalil and M. Bayoumi, "Affine Invariants for Object Recognition Using the Wavelet Transform," *Pattern Recognition Letters*, vol. 23, pp. 57-72, 2002.

[32] M. Khalil and M. Bayoumi, "A Dyadic Wavelet Affine Invariant Function for 2-D Shape Recognition," *IEEE Trans. Pattern Analysis and Machine Intelligence*, vol. 23, no. 10, pp. 1152-1164, Oct. 2001.

[33] E. Bala and A. Cetin, "Computationally Efficient Wavelet Affine Invariant Functions for Shape Recognition," *IEEE Trans. Pattern Analysis and Machine Intelligence*, vol. 26, no. 8, pp. 1095-1099, Aug. 2004.

[34] *An Introduction to Wavelets*, vol. 1 of *Wavelet Analysis and Its Applications*, C. Chui, ed. Academic Press, 1992.

[35] *Wavelet Theory and Its Application to Pattern Recognition*, vol. 36 of *Machine Perception and Artificial Intelligence*, Y. Tang, L. Yang, J. Liu, and H. Ma, eds. World Scientific, 2000.